A Low-Overhead Interference Canceller for High-Mobility STBC-OFDM Systems

Hsiao-Yun Chen, Wei-Kai Chang, and Shyh-Jye Jou

***Abstract*—This paper proposes a low-overhead space-time block code (STBC) interference canceller for high-mobility STBC-orthogonal frequency division multiplexing (STBC-OFDM) systems. The proposed STBC interference canceller combined with the two-stage channel estimator can be applied to wireless metropolitan area network (WMAN), like IEEE 802.16e system. At the vehicle speeds of 240 km/hr for 16 quadrature amplitude modulation (16 QAM), the bit error rate (BER)can be improved about 10 times of that just using the two-stage channel estimator. The proposed design is implemented in 90 nm CMOS technology. The gate count is 109.3 K, and the power dissipation is 1.45 mW at 83.3 MHz operation frequency with 1 V power supply. However, up to 61% hardware can be reused from the existed two-stage channel estimator design. After reusing, the proposed STBC interference canceller requires only 42.2 K gates, which is 4.9% overhead of the two-stage channel estimator.**

***Index Terms*—Data detection, interference canceller, STBC-OFDM, WMAN.**

I. Introduction

WIRELESS metropolitan area network (WMAN), allowing end-users to travel throughout a hot zone cell without losing connectivity, has been a very important technique in wireless communication. The high-quality services provide portability and mobility to make users more convenient to access information. The orthogonal division multiple access (OFDMA) technique is adopted in WMAN standards to support multiple-input multiple-output (MIMO) systems and multiple access scheme over multipath fading channels. However, the mobile channel often varies rapidly, which is caused by a large Doppler spread, particularly when the mobile station (MS) moves at the vehicular speed. A fundamental phenomenon that makes credible wireless transmission expensive and difficult is time-varying multipath channels. In order to improve the transmission quality in fast and selective fading channels, transmit diversity is an effective technology for reducing fading effect in mobile wireless communication, especially when receive diversity is expensive or impractical to acquire. In recent years, space-time block code (STBC) has been shown to give high code rate and good performance. It can be applied in orthogonal frequency division multiplexing (OFDM) systems with multiple antennas to provide better performance by exploiting transmit diversity, and it was also supported by WMAN standards. Nevertheless, STBC-OFDM systems are sensitive to the temporal channel variation within a code word since the symbols within one code word interfere with each other. Besides, time-varying multipath channels introduce inter-carrier interference (ICI) among the OFDM subcarriers. These interference noises degrade the STBC-OFDM system performance. Hence, an STBC interference cancellation scheme is required for better performance when the detailed channel state information (CSI) variation is unavailable.

In this paper, the design and implementation of an STBC interference canceller for high-mobility WMAN are proposed. The implementation uses IEEE 802.16e standard as a test platform. IEEE 802.16e is an extension of IEEE 802.16-2004 for providing high data rate transmission and mobility of WMAN [1], [2]. It enables mobile speed up to 120 km/hr but is also backward compatible to support the fixed mode. This design has lower computational complexity and better performance as compared with other previous researches [3]–[6]. By using 90 nm CMOS technology, this design has about 109.3 K gates and dissipates 1.45 mW at 83.3 MHz operating frequency. However, most of the hardware in the proposed design can be reused from the existed two-stage channel estimator design [8]. After reusing, the area can be reduced to 42.2 K gates. It is only 4.9% overhead of the two-stage channel estimator. The proposed data detection design includes the following achievements:

- development of an low-complexity STBC interference cancellation algorithm for high-mobility STBC-OFDM systems;
- implementation of an efficient STBC interference canceller;
- integration of the proposed STBC interference canceller andthe existed two-stage channel estimator with only 4.9% overhead.

This paper is organized as follows. Section II describes the system architecture. Section III briefly reviews the two-stage channel estimator and introduces the proposed interference cancelling data detection method. Section IV presents the proposed STBC interference canceller. Then, the simulations and the design results are provided in Section V. Finally, Section VI is the conclusions.

Notation: The superscript $(.)^*$ stands for complex conjugate; $(.)^T$ denotes transpose; $(.)^H$ denotes Hermintian transpose. The notation $|.|$ denotes the absolute value. The notation $\lfloor . \rfloor$ denotes

Manuscript received August 24, 2012; revised December 27, 2012; accepted January 17, 2013. Date of publication March 18, 2013; date of current version September 25, 2013. This work was supported by the UMC, CIC, and the National Science Council of Taiwan, R.O.C. This paper was recommended by Associate Editor M. Sanduleanu.

The authors are with the Department of Electronics Engineering, National Chiao Tung University, Hsinchu 30010, Taiwan, R.O.C. (e-mail: jerryjou@mail.nctu.edu.tw).

Color versions of one or more of the figures in this paper are available online at http://ieeexplore.ieee.org.

Digital Object Identifier 10.1109/TCSI.2013.2248831

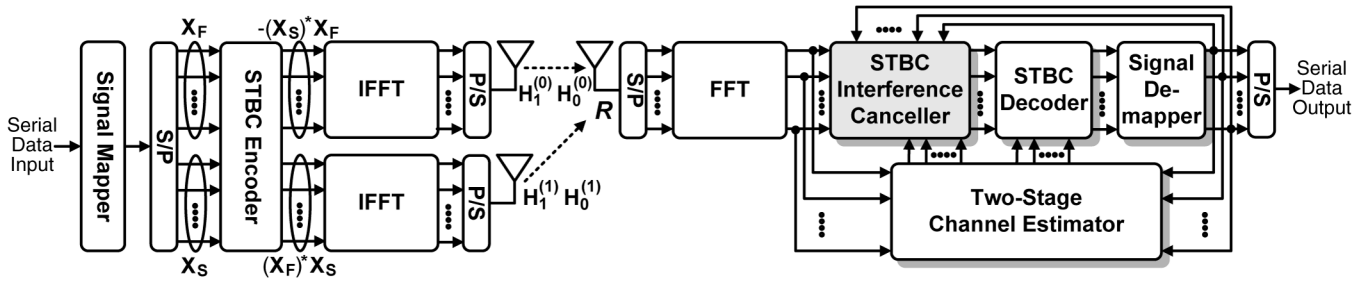

Fig. 1. Proposed STBC-OFDM system with two transmit antennas and one receive antenna.

TABLE I
MAJOR PARAMETERS OF THE PROPOSED STBC-OFDM SYSTEM

Parameters		Values
RF frequency		2.5 GHz
FFT size (N)		1024
Cyclic Prefix Length (N_g)		128
System channel bandwidth (BW)		10 MHz
Sampling frequency (F_s)		11.9 MHz
Subcarrier spacing (Δf)		10.94 kHz
Useful symbol time (T_b)		91.4 us
Frame duration (T_F)		5 ms
DL PUSC	Number of null subcarriers (N_n)	184
	Number of pilot subcarriers (N_p)	120
	Number of data subcarriers (N_d)	720
Number of OFDM data in a frame		40

the floor function. The notation $(.)_N$ performs modulo-N operation. In general, an italic letter stands for a number; a bold letter stands for a matrix or a set; a bold and italic letter stands for a vector; an upper case letter denotes a frequency-domain signal; a lower case letter denotes a time-domain signal. $\mathbf{S}[:, a]$ stands for the a-th column of matrix $\mathbf{S}$ while $\mathbf{S}[b, :]$ stands for the b-th row. $\mathbf{J} = \{J_0, J_1, \cdots, J_{N_j-1}\}$ represents the pilot subcarrier index set, and N_j denotes the number of elements inside the pilot index set $\mathbf{J}$. Based on the same principle, $\boldsymbol{\Theta}$ represents the data subcarrier index set.

II. SYSTEM ARCHITECTURE

The OFDMA specification of IEEE 802.16e that supports the multi-antenna technology is adopted in this paper. The subcarrier allocation of partial usage of subchannels (PUSC) in downlink (DL) transmission is supported in this proposed system. The major parameters of the proposed STBC-OFDM system are summarized in Table I. The quadrature phase shift keying (QPSK) and 16 quadrature amplitude modulation (16 QAM) are supported for data subcarriers, while binary phase shift keying (BPSK) is adopted for pilot subcarriers and preamble symbols. Each frame is composed of one preamble symbol and 40 OFDM data symbols. The cyclic prefix (CP) length is 128 sampling periods, i.e., 1/8 of the useful symbol time.

The proposed STBC-OFDM system with two transmit antennas and one receive antenna is shown in Fig. 1. In the transmitter, Alamouti's STBC encoding method is used to encode two transmitted symbols, $\boldsymbol{X_F}$ and $\boldsymbol{X_S}$, within a time slot which is the duration of two OFDM symbols. Note that the guard interval insertion, guard interval removal, digital-to-analog converter, analog-to-digital converter, carrier recovery, timing recovery, and front-end components are omitted in Fig. 1 for simplicity. The receiver architecture consists mainly of a two-stage channel estimator and an STBC interference canceller along with other blocks. Without loss of generality, the signal processing of the received data is focused on each time slot, and the time slot index is omitted hereafter except otherwise stated.

Let $X[k]$ be the k-th subcarrier of an OFDM symbol, which can carrier the pilot or data symbol. After N-point inverse fast Fourier transform (IFFT) and appending cyclic prefix with length N_g, the transmitted time-domain data symbol at the n-th sample is denoted as

$$x[n] = \frac{1}{N}\sum_{k=0}^{1} X[k]e^{j\frac{2\pi kn}{N}}, n \in \{-N_g, -N_g+1, \cdots, N-1\} \tag{1}$$

Assuming the multipath fading channel between the a-th transmit antenna, for $a \in \{0, 1\}$, and the receive antenna is made of L discrete paths. The received signal can be expressed as [9]

$$r_b^{(a)}[n] = \sum_{l=0}^{L-1} h_{b,l}^{(a)}[n]x[n-\tau_l] + z_b[n] \tag{2}$$

where $h_{b,l}^{(a)}[n]$ represents the complex path gain for the l-th path at the n-th sample within the b-th symbol interval of a time slot, for $b \in \{0, 1\}$, and τ_l denotes the delay of the l-th path. $z_b[n]$ denotes a circularly symmetric zero-mean white Gaussian random noise. By removing the cyclic prefix and taking the fast Fourier transform (FFT), the received signal in frequency domain is given by

$$\begin{aligned} R_b[k] &= \sum_{a=0}^{1}\sum_{m=0}^{N-1}\sum_{l=0}^{L-1}\left\{X[m]e^{-j\frac{2m\tau_l}{n}} \cdot \frac{1}{N}\sum_{n=0}^{N-1} h_{b,l}^{(a)}[n]e^{j\frac{2\pi n(m-k)}{N}}\right\} \\ &\quad + Z_b[k] \\ &= \sum_{a=0}^{1}\sum_{m=0}^{N-1} H_b^{(a)}[k,m]X[m] + Z_b[k] \end{aligned} \tag{3}$$

$$H_b^{(a)}[k,m] = \frac{1}{N}\sum_{l=0}^{L-1}\left\{e^{-j\frac{2m}{N}\tau_l} \cdot \sum_{n=0}^{N-1} h_{b,l}^{(a)}[n]e^{j\frac{2\pi n(m-k)}{N}}\right\} \tag{4}$$

where $H_b^{(a)}[k,m]$ represents the frequency-domain channel matrix from the m-th transmitted subcarrier to the k-th received subcarrier for $k,m = 0,1,\cdots,N-1$ Note that $H_b^{(a)}[k,m],\ \forall k \neq m$ stands for the ICI caused by Doppler spread, and the diagonal entries $H_b^{(a)}[k,m],\ \forall k \neq m$, denotes the channel frequency response (CFR).

If the system operates under stationary environment, the temporal variation of wireless multi-path channel is not significant within any two successive OFDM symbol durations. This quasi-static condition is the basic assumption of Alamouti's STBC scheme. However, if the system operates under highly-mobile environment, the quasi-static condition no longer holds because of rapid channel variation, and severe interference is introduced in Alamouti's STBC decoding method. More details of Alamouti's STBC scheme under these two environments are described as follows.

A. Quasi-Static Channel

If the channel is quasi-static within a time slot, the complex path gain is almost fixed within two OFDM symbol time, and the ICI terms are negligible.

$$h_{b,l}^{(a)}[n] \cong \overline{h}_l^{(a)} = \frac{1}{2N}\sum_{b=0}^{1}\sum_{n=0}^{N-1} h_{b,l}^{(a)}[n] \tag{5}$$

$$\begin{aligned} H_0^{(a)}[k,m] &\cong H_1^{(a)}[k,m] \\ &\cong \begin{cases} \widetilde{H}^{(a)}[k] \triangleq \sum\limits_{l,0}^{L-1} \overline{h}_l^{(a)} e^{-j2\frac{k}{N}\tau_l}, & if\ k=m \\ 0, & if\ k \neq m \end{cases} \end{aligned} \tag{6}$$

where $\overline{h}_l^{(a)}$ denotes the l-th approximated path gain of a time slot. $\widetilde{H}^{(a)}$ stands for the channel frequency response over one time slot duration.

Then, the received signal $\boldsymbol{R}[k]$ with two received OFDM symbols $R_0[k]$ and $R_1[k]$ in a time slot can be arranged as

$$\boldsymbol{R}[k] = \widetilde{\mathbf{A}}[k]\boldsymbol{X}[k] + \boldsymbol{Z}[k] \tag{7}$$

where

$$\boldsymbol{R}[k] = \begin{bmatrix} R_0[k] \\ (R_1[k])^* \end{bmatrix} \tag{8}$$

$$\widetilde{\mathbf{A}}[k] = \begin{bmatrix} \widetilde{H}^{(0)}[k] & \widetilde{H}^{(1)}[k] \\ \left(\widetilde{H}^{(1)}[k]\right)^* & -\left(\widetilde{H}^{(0)}[k]\right)^* \end{bmatrix} \tag{9}$$

$$\boldsymbol{X}[k] = \begin{bmatrix} X_F[k] \\ X_S[k] \end{bmatrix} \tag{10}$$

$$\boldsymbol{Z}[k] = \begin{bmatrix} Z_0[k] \\ (Z_1[k])^* \end{bmatrix}. \tag{11}$$

According to STBC decoding method, the decoded symbols $\hat{X}^F[k]$ and $\hat{X}^s[k]$ can be expressed as

$$\widehat{\boldsymbol{X}}[x] = \begin{bmatrix} \hat{X}_F[k] \\ \hat{X}_S[k] \end{bmatrix} = Dec\left\{ \frac{1}{\sigma[k]} \cdot \widetilde{\mathbf{A}}^H[k]\boldsymbol{R}[k] \right\} \tag{12}$$

where $Dec\{\cdot\}$ is the decision process and

$$\sigma[k] = \left|\widetilde{H}^{(0)}[k]\right|^2 + \left|\widetilde{H}^{(1)}[k]\right|^2. \tag{13}$$

As a result, the two encoded symbols can be recovered without any coupling interference if the quasi-static condition holds during a time slot.

B. Highly-Mobile Channel

If the system operates under highly-mobile environment, the quasi-static condition in (5) and (6) fails. The received signals in (7) should be re-expressed as

$$\begin{aligned} \boldsymbol{R}[k] &= \sum_{m=0}^{N-1} \mathbf{A}[k,m]\boldsymbol{X}[m] + \boldsymbol{Z}[k] \\ &= \widetilde{\mathbf{A}}[k]\boldsymbol{X}[k] + (\boldsymbol{I}_{CCI}[k] + \boldsymbol{I}_{ICI}[k] + \boldsymbol{I}_{ICI,\Delta}[k]) \\ &\quad + \boldsymbol{Z}[k] \end{aligned} \tag{14}$$

where

$$\boldsymbol{I}_{CCI}[k] = \mathbf{A}_\Delta[k,m]\boldsymbol{X}[k], \quad \forall k = m \tag{15}$$

$$\boldsymbol{I}_{ICI}[k] = \sum_{m=0,m\neq \mathrm{k}}^{N-1} \overline{\mathbf{A}}[k,m]\boldsymbol{X}[m] \tag{16}$$

$$\boldsymbol{I}_{ICI,\Delta}[k] = \sum_{m=0,\mathrm{m}\neq \mathrm{k}}^{N-1} \mathbf{A}_\Delta[k,m]\boldsymbol{X}[m] \tag{17}$$

$$\mathbf{A}[k,m] = \begin{bmatrix} H_0^{(0)}[k,m] & H_0^{(1)}[k,m] \\ \left(H_1^{(1)}[k,m]\right)^* & -\left(H_1^{(0)}[k,m]\right)^* \end{bmatrix} \tag{18}$$

$$\overline{\mathbf{A}}[k,m] = \begin{bmatrix} \overline{H}^{(0)}[k,m] & \overline{H}^{(1)}[k,m] \\ \left(\overline{H}^{(1)}[k,m]\right)^* & -\left(\overline{H}^{(0)}[k,m]\right)^* \end{bmatrix} \tag{19}$$

$$\mathbf{A}_\Delta[k,m] = \mathbf{A}[k,m] - \overline{\mathbf{A}}[k,m] \tag{20}$$

$$\mathbf{A}[k,k] = \widetilde{\mathbf{A}}[k] \tag{21}$$

$$\overline{H}^{(a)}[k,m] = \frac{1}{2}\sum_{b=0}^{1} H_b^{(a)}[k,m]. \tag{22}$$

As compared with (7), the time-variant channel introduces three interference noises on the right-hand side of (14). $\boldsymbol{I}_{CCI}$ acts as the co-carrier interference (CCI) because it couples between two encoded symbols of the same subcarrier. $\boldsymbol{I}_{ICI}$ and $\boldsymbol{I}_{ICI,\Delta}$ are both ICI, but their difference is that $\boldsymbol{I}_{ICI,\Delta}$ couples between $X_F[k]$ and $X_s[k]$ symbol vectors while does not. The presence of these three interference components in time-varying channels results in severe performance degradation.

It has been studied that CCI problem is more important than ICI problems, and simulation results provided in [4] shows that the CCI power is larger than the ICI power by $7 \sim 8$ dB regardless of the channel variation rate.

III. Interference Cancelling Data Detection Method

In order to mitigate the impact of CCI and ICI, various approaches have been studied in [3]–[6]. In [4], a successive interference cancellation (SIC) and least squares (LS) method were proposed. In [6] the maximum likelihood (ML) method was used to deal with CCI problem. In [3], a modified ML method was proposed to reduce the complexity of traditional ML method. Most of the previous works do not use STBC decoding technique; instead, they use other sophisticated data

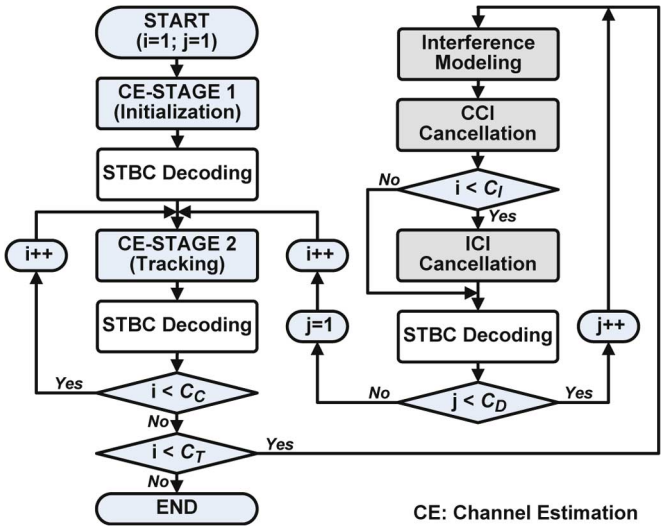

Fig. 2. Proposed data detection flow.

detection methods. However, these data detection methods result in a significant hardware overhead.

One design target of this paper is to integrate the interference cancellation algorithm with an existed two-stage channel estimator [8]. Under limited clock cycles and hardware budget, we use the Alamouti's STBC decoding technique and focus on modeling interference noise components. Based on the method in [5], the data detection flow is described in Fig. 2, where j stands for the iteration count of the interference cancellation and i stands for the iteration count of the data decision. The parameters of C_T, C_C, C_I, and C_D represent four control values in the proposed data detection flow.

A. Channel Estimation

Various DFT-based channel estimation method has been studied using either minimum mean square error (MMSE) criterion or ML criterion for OFDM system with preambles [10], [11]. Since CSI and signal to noise ratio (SNR) are unavailable at receiver in real implementation, the ML scheme is easier to implement than MMSE scheme. Moreover, the decision-feedback (DF) scheme can be adopted in DFT-based channel estimation to use decision data as pilot to track channel variations for providing sufficient tracking information. Recently, Ku and Huang [12] presented a two-stage channel estimation method for STBC-OFDM systems under fast time-varying multipath channels. They concluded that a refined two-stage channel estimator is more robust than classical DFT-based method. An initialization stage uses a multipath interference cancellation (MPIC)-based decorrelation method to identify the significant paths of channel impulse response (CIR) in the beginning of each frame. However, the CIR estimated by the preamble cannot be directly applied in the following data bursts since the channel is time-variant. Thus, a tracking stage is then used to track the path gains with known CIR positions.

B. STBC Interference Canceller

1) Co-Carrier Interference Modeling: $\boldsymbol{I}_{CCI}$ is resulted from channel variation between two symbol intervals within one time slot. Various studies had demonstrated that CCI is the major impact on STBC-OFDM systems [3]–[6], so CCI cancellation shall be done before ICI cancellation in our proposed algorithm.

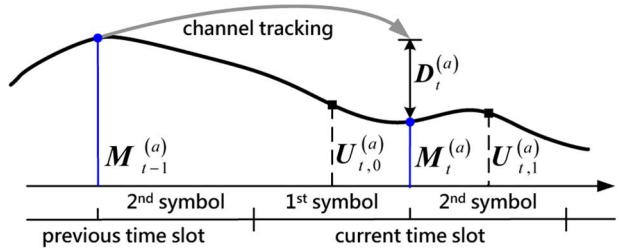

Fig. 3. Relationship between the estimated CFRs.

To calculate CCI noise, we need to know the CFRs of different transmission antenna pairs, i.e. $H_b^{(a)}[k,m],\ \forall k = m, a, b \in \{0,1\}$. Nevertheless, most channel estimators designed for STBC-OFDM systems are aimed to estimate the averaged CFR over two symbol intervals such as $\overline{H}^{(a)}[k,m],\ \forall k = m$, in (22). The goal of this paper is to provide an efficient interference cancellation solution for STBC-OFDM systems. Therefore, we propose an algorithm using only the time-slot based CFR estimation to approximate the CFRs of two symbol intervals within a time slot.

The study in [7] had proved that the averaged CFR over a duration approaches to the CFR taken in the middle of the duration. Based on [7], Fig. 3 demonstrates the relationship between CFR tracking estimations in time domain, where $\boldsymbol{M}_t^{(a)}$ denotes the estimated CFR of a-th transmit antenna during the t-th time slot, and $\boldsymbol{D}_t^{(a)} = \boldsymbol{M}_{t-1}^{(a)} - \boldsymbol{M}_t^{(a)}$ denotes the tracking-update value calculated by the two-stage channel estimator [8]. $\boldsymbol{U}_{t,b}^{(a)}$ represents our approximated CFR of the a-th transmit antenna during the b-th symbol interval. We notice that no matter which method is used to obtain $\boldsymbol{U}_{t,b}^{(a)}$, but the following constraint must be held

$$\frac{1}{2}\left(\boldsymbol{U}_{t,0}^{(a)} + \boldsymbol{U}_{t,1}^{(a)}\right) = \boldsymbol{M}_t^{(a)}. \tag{23}$$

A low cost solution for getting $\boldsymbol{U}_{t,0}^{(a)}$ is to interpolate the existed information, $\boldsymbol{M}_t^{(a)}$ and $\boldsymbol{M}_{t-1}^{(a)}$. The estimation of $\boldsymbol{U}_{t,1}^{(a)}$, is non-causal for real implementation, so several predictive approaches have been studied [13].

In the study of [13], three predictive models using only previous estimated information are proposed for time-varying channel. They concluded that the 1st-order predictive model and linear extrapolation have better performance under time-varying channel. Moreover, by applying the 1st-order predictive model on $\boldsymbol{U}_{t,1}^{(a)}$, we can interpolate $\boldsymbol{U}_{t,0}^{(a)}$ simultaneously without violating the constraint in (23). As a result, our proposed approximation is given by

$$\boldsymbol{U}_{t,0}^{(a)} = 0.75 \cdot \boldsymbol{M}_t^{(a)} + 0.25 \cdot \boldsymbol{M}_{t-1}^{(a)} \tag{24}$$

$$\boldsymbol{U}_{t,1}^{(a)} = 1.25 \cdot \boldsymbol{M}_t^{(a)} - 0.25 \cdot {}^{(a)}_{t-1}. \tag{25}$$

2) Inter-Carrier Interference Modeling: In time-varying channel, CCI component is more significant than ICI component in STBC-OFDM systems. As a result, other studies for STBC interference cancellation target only on CCI and ignore

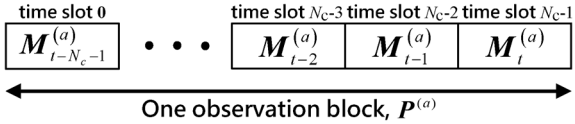

Fig. 4. Diagram of one observation block.

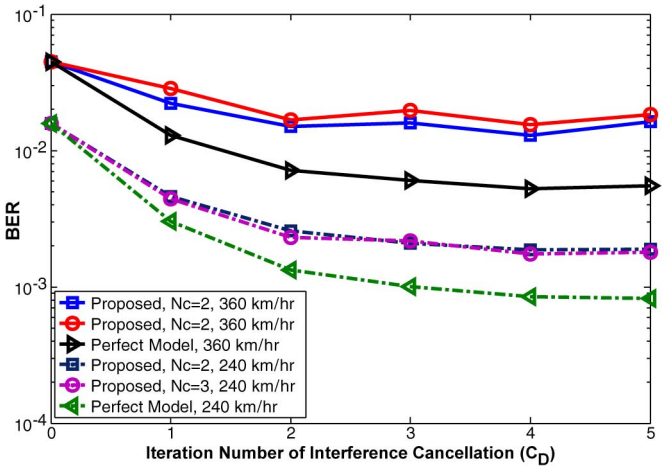

Fig. 5. BER performances versus the decoding iteration number for 16 QAM at the vehicle speed 240 km/hr and 360 km/hr.

ICI problem [3]–[6]. In this section, we propose a low-complexity algorithm to model ICI by exploiting the information used for CCI modeling. In this way, CCI and ICI noise can be cancelled simultaneously with little overhead. The ICI component $\boldsymbol{I}_{ICI,\Delta}$ is much smaller than $\boldsymbol{I}_{ICI}$ and is very difficult to be estimated accurately from the available time-slot based estimated CFR $\overline{\mathbf{H}}^{(a)}$; hence, we ignore $\boldsymbol{I}_{ICI,\Delta}$ and focus on modeling I_{ICI} only.

The estimation of $\overline{\mathbf{A}}[k,m]$ defined in (19) requires the temporal path gain variation in each symbol interval, but the channel estimator provides only the temporal averaged CSI of a time slot. We adopt a LS fitted polynomial method [14]–[16] to model the detail of the l-th complex path gain as follows.

$$\mu_l^{(a)}[n] = \sum_{d=0}^{N_c-1} \kappa^{(a)}[l,d] \cdot n^d + \varepsilon_l^{(a)}[n] \tag{26}$$

where $\mu_l^{(a)}[n]$ represents the modeled complex path gain at time sample index n, $\kappa^{(a)}[l,d]$ is the l-th path and the d-th order LS fitting polynomial coefficient in time domain, $d \in \{0,1,\cdots,N_c-1\}$, $\varepsilon_l^{(a)}[n]$ stands for modeling error, and (N_c-1) denotes the order of the LS fitting polynomial. It requires N_c observations to solve this (N_c-1)-th order LS fitting problem, so we consider the estimated CFRs in N_c time slots and group them as an observation block for each ICI modeling computation. As illustrated in Fig. 4, an observation block is composed of N_c time slots where the latest estimated CFR is in the (N_c-1)-th time slot. Then, by combining(26) with the frequency-domain channel matrix (4), we have

$$\overline{\mathbf{G}}^{(a)} = \frac{1}{2}\sum_{b=0}^{1} \mathbf{G}_b^{(a)} = \sum_{d=0}^{N_c-1} diag\left\{\mathbf{Q}^{(a)}[:,d]\right\} \cdot \boldsymbol{\Psi}_d \tag{27}$$

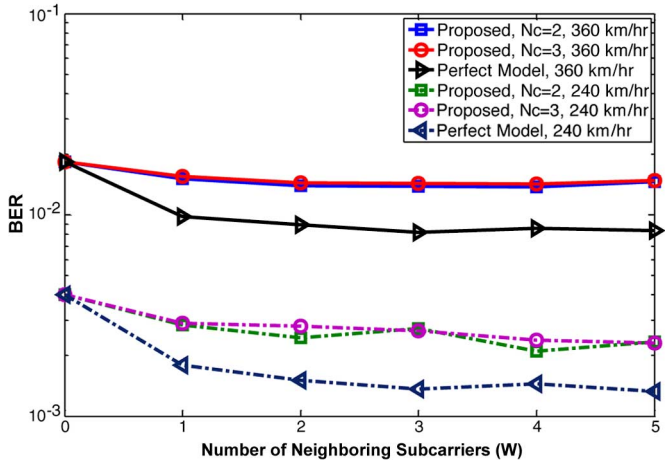

Fig. 6. BER performances versus the ICI subcarrier number for 16 QAM at the vehicle speed 240 km/hr and 360 km/hr.

where $\mathbf{G}_b^{(a)}$ and $\overline{\mathbf{G}}^{(a)}$ are the estimated channel matrix of $\mathbf{H}_b^{(a)}$ and $\overline{\mathbf{H}}^{(a)}$, respectively. Two parts decomposed from $\overline{\mathbf{G}}^{(a)}$ are defined as

$$Q^{(a)}[m,d] = \sum_{l=0}^{L-1} \kappa^{(a)}[l,d] \cdot e^{-j2\pi\frac{m}{N}\tau_l} \tag{28}$$

$$\psi_d[k,m] = \frac{1}{2N}\sum_{n=0}^{N-1}\left(\sum_{b=0}^{1}\left(N_g+(2N_c-2+b)N_s+q\right)^d\right) \cdot e^{j2\pi\frac{m-k}{N}n} \tag{29}$$

where $\boldsymbol{\Psi}_d$ is a constant matrix that can be pre-computed, and $N_s = N_g + N$. $\mathbf{Q}^{(a)}$ denotes the LS fitting polynomial coefficient matrix in frequency domain and is given by

$$\mathbf{Q}^{(a)} = \mathbf{P}^{(a)} \cdot \mathbf{T}^{(-1)} \tag{30}$$

where

$$\mathbf{P}^{(a)} = \begin{bmatrix} \boldsymbol{M}^{(a)}_{t-N_c+1} & \cdots & \boldsymbol{M}^{(a)}_{t-1} & \boldsymbol{M}^{(a)}_{t} \end{bmatrix} \tag{31}$$

$$T[r,s] \triangleq \frac{1}{2N}\left(\sum_{n=(2s)}^{(2s+1)\cdot N_s-1} n^r + \sum_{n=(2s+1)\cdot N_s+N_g}^{(2s+2)\cdot N_s-1} n^r\right) \tag{32}$$

and $r,s \in \{0,1,\cdots,N_c-1\}$. $\mathbf{P}^{(a)}$ is the observation block as illustrated in Fig. 4.

Fig. 5 shows the BER performance of the proposed algorithm with the different iteration number of the interference cancellation C_D, as defined in Fig. 2, for 16 QAM modulations at the vehicle speed of 240 km/hr and 360 km/hr. In the case of $C_D = 0$, the interference cancellation is not applied. Fig. 6 shows the BER performance of the proposed CCI and ICI modeling with the different number of the neighboring ICI subcarriers (W). For example, $W = 5$ represents ten neighboring subcarriers are considered for ICI modeling. In the case of $W = 0$, ICI noises are ignored, and only CCI cancellation is applied. In order to focus on the effect of CCI and ICI noises, the ratio of received bit energy to the noise power spectral density $\mathrm{E_b/N_0}$ is set to be 30 dB in these simulations. Fig. 5 and Fig. 6 show that the curves get into saturation at $C_D = 2$ and $W = 2$. Moreover, the

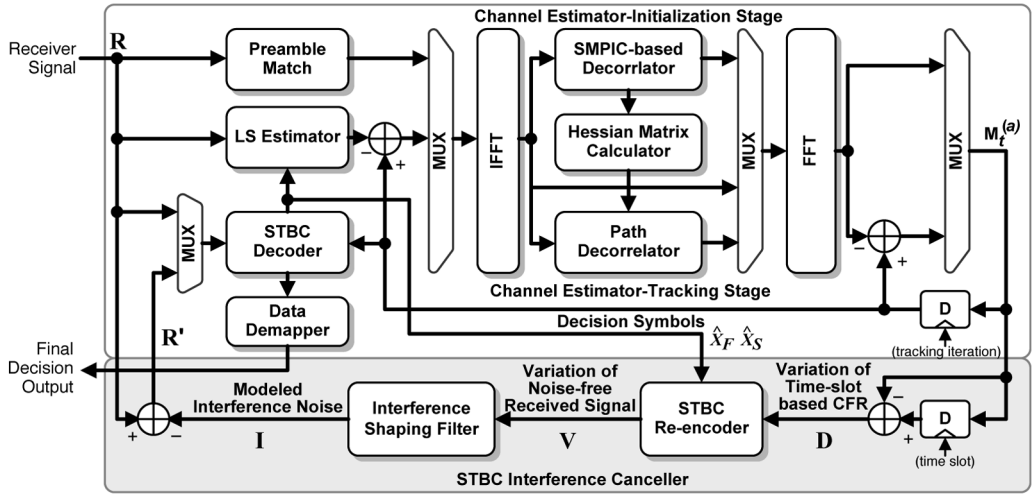

Fig. 7. Architecture of the proposed STBC interference canceller.

2nd-order ICI modeling doesn't outperform the 1st-order modeling. By considering the design cost and the performance, we adopt the 1st-order ICI modeling with four neighboring subcarriers ($N_c = 2; W = 2$) and execute two interference cancellation iteration ($C_D = 2$) in the proposed design.

IV. Proposed STBC Interference Canceller

Fig. 7 shows the architecture of the proposed STBC interference canceller with the two-stage channel estimator. Based on the two-stage channel estimation method studied in [12], a low complexity and robust implementation was proposed by [8]. The initialization stage is decomposed to a preamble match, an IFFT, a straight MPIC (SMPIC)-based decorrelator, and an FFT. The tracking stage is decomposed to a STBC decoder, a demapper, an LS estimator, a FFT, a path decorrelator, a Hessian matrix calculator, and an IFFT. Moreover, the IFFT and FFT are shared between the initialization stage and the tracking stage.

In the proposed STBC interference canceller, the STBC re-encoder exploits the estimated CFR variation ($\mathbf{D}$) and the decision symbols to generate the variation of noise-free received signal ($\mathbf{V}$) within a time slot. Based on the received signal variation of a subcarrier, the interference shaping filter approximates the CCI noise introduced into this subcarrier and the ICI noise spreading to other subcarriers. Then, the interference noises of this subcarrier are accumulated. Finally, the estimated interference ($\mathbf{I}$) is cancelled from the actual received signal ($\mathbf{R}$), and this refined received signal ($\mathbf{R}'$) is fed into the STBC decoder to get better decision symbols.

The signal processing flow is presented in Fig. 8. The white blocks in Fig. 8 (e.g.the memory used to store the latest estimated CFRs, the memory holding the received signals, the pilot read-only memory (ROM), the STBC decoder, and the demapper)can be reused from the channel estimator hardware [8]. Only the gray blocks are required for implementation. This process only needs the $2W$ neighboring subcarriers that induce the significant ICI noise into the central subcarrier. Since the constellation values are known, we store the demapped binary bit values of the decision symbols instead of their complex

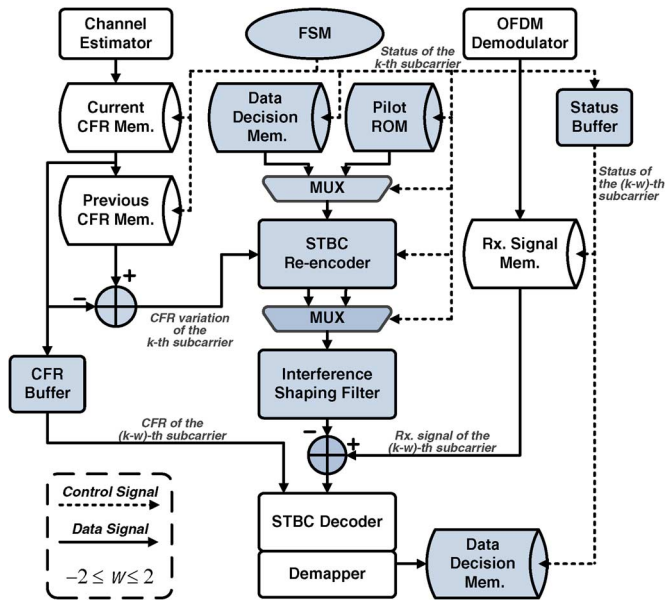

Fig. 8. Operation flow of the proposed STBC interference canceller.

values to save the memory size. The details of key blocks will be described in the following sections.

A. Simplification of the Proposed Algorithms

1) CCI Noise: According to the approximation models derived in (15) and (24), (25), the CCI noise estimation can be formulated as

$$\hat{\boldsymbol{I}}_{CCI}[k] = \begin{bmatrix} 0.25 & 0 \\ 0 & -0.25 \end{bmatrix} \boldsymbol{V}[k] \tag{33}$$

$$\begin{aligned} \boldsymbol{V}[k] &= \begin{bmatrix} V_0[k] \\ V_1[k] \end{bmatrix} \\ &\triangleq \begin{bmatrix} D_t^{(0)}[k] & D_t^{(1)}[k] \\ \left(D_t^{(1)}[k]\right)^* & -\left(D_t^{(0)}[k]\right)^* \end{bmatrix} \widehat{\boldsymbol{X}}[k] \end{aligned} \tag{34}$$

$$\boldsymbol{D}_t^{(a)} = \boldsymbol{M}_{t-1}^{(a)} - \boldsymbol{M}_t^{(a)} \tag{35}$$

where $\hat{\boldsymbol{I}}_{CCI}$ denotes the modeled CCI noise and $k \in \boldsymbol{\Theta}$.

2) ICI From Data Subcarriers: According to (27), the estimated CFR matrix is composed of constant matrix $\boldsymbol{\psi}_d$ which models the shape of Doppler spread and the variable part $diag\{\mathbf{Q}^{(a)}[:,d]\}$ which is transformed from the observed CFRs. We further combine the linear transformation $\mathbf{T}^{(-1)}$ with $\boldsymbol{\psi}_d$ to obtain a new matrix $\boldsymbol{\Phi}$ which has the constant entries and can be precomputed. The final expression of averaged CFR matrix is given by

$$\bar{G}^{(a)}[k,m] = \begin{cases} \left(M_{t-1}^{(a)}[k] - M_t^{(a)}[k]\right) \Phi[k,m], & if\ k \neq m \\ M_t^{(a)}[k], & if\ k = m \end{cases} \tag{36}$$

where

$$\Phi[k,m] = \begin{cases} \frac{E}{N} \sum_{q=0}^{N-1} n \cdot e^{j2\pi \frac{m-k}{N} n}, & if\ k \neq m \\ \frac{(N-1)}{2}, & if\ k = m \end{cases} \tag{37}$$

$$E = T^{-1}[0,0] + (3.5N_s) \cdot T^{-1}[0,1] \tag{38}$$

for $k, m \in \boldsymbol{\Theta}$. As a result, the ICI from data subcarriers can be estimated as

$$\hat{\boldsymbol{I}}_{ICI}[k] = \sum_{\substack{m \\ m \in \Theta \setminus \{k\}}} \begin{bmatrix} \Phi[k,m] & 0 \\ 0 & (\Phi[k,m])^* \end{bmatrix} \boldsymbol{V}[m]. \tag{39}$$

3) ICI From Pilot Subcarriers: Both the transmitted data subcarriers and the pilot subcarriers contribute ICI noise to the received data subcarriers. As a result, our proposed design takes pilot ICI noise into account. The detail of pilot insertion in our system was described in [8]. The pilots do not pass through the STBC encoding before transmission, so the pilot ICI estimation is given by

$$\hat{\boldsymbol{I}}_{ICI,P}[k] = \sum_{g=0}^{\frac{N_J}{2}-1} \begin{bmatrix} P[g] \left(\bar{G}^{(0)}[k, J_{2g+1}] + \bar{G}^{(1)}[k, J_{2g}]\right) \\ (P[g])^* \left(\bar{G}^{(0)}[k, J_{2g}] + \bar{G}^{(1)}[k, J_{2g+1}]\right)^* \end{bmatrix} \tag{40}$$

where $\hat{\mathbf{I}}_{ICI,P}$ represents the estimated pilot ICI noise, $P[g]$ denotes the pilot symbol at the g-th pilot subcarrier, $g \in \boldsymbol{J}$.

4) Joined Interference Modeling: It can be observed that $\Phi[k,m]$ depends on the value of $|k-m|$. If we define the interference shaping coefficients as

$$S_0\left[|k-m|\right] = \begin{cases} \Phi[k,m], & if\ k \neq m \\ 0.25, & if\ k = m \end{cases} \tag{41}$$

$$S_1\left[|k-m|\right] = \begin{cases} (\Phi[k,m])^*, & if\ k \neq m \\ -0.25, & if\ k = m \end{cases} \tag{42}$$

then (33) and (39) can be combined together as

$$\hat{\boldsymbol{I}}_{CCI}[k] + \hat{\boldsymbol{I}}_{ICI}[k] = \sum_{\substack{m \\ m \in \boldsymbol{\Theta}}} \begin{bmatrix} S_0\left[|k-m|\right] & 0 \\ 0 & S_1\left[|k-m|\right] \end{bmatrix} \boldsymbol{V}[m]. \tag{43}$$

Based on [9], ICI noise only needs to consider the neighboring subcarriers $2W$ when the normalized maximum Doppler frequency is small (less than 0.1). Therefore, we modify (43) to

$$\hat{\boldsymbol{I}}_{CCI}[k] + \hat{\boldsymbol{I}}_{ICI}[k] \cong \sum_{\substack{w=-W \\ (k+w)_N \in \boldsymbol{\Theta}}}^{W} \begin{bmatrix} S_0\left[|w|\right] & 0 \\ 0 & S_1\left[|w|\right] \end{bmatrix} \boldsymbol{V}\left[(k+w)_N\right]. \tag{44}$$

Similarly, $\hat{\boldsymbol{I}}_{ICI,P}$ can be reformulated as follows

$$\begin{aligned} \hat{\boldsymbol{I}}_{ICI,P}[k] \cong & \sum_{\substack{u=-W \\ m_u = J_{2g}}}^{W} \begin{bmatrix} S_0\left[|u|\right] & 0 \\ 0 & S_1\left[|u|\right] \end{bmatrix} \begin{bmatrix} D_t^{(1)}[m_u] \\ \left(D_t^{(0)}[m_u]\right)^* \end{bmatrix} \\ & \times P\left[\left\lfloor \frac{m_u}{2} \right\rfloor\right] \\ & + \sum_{\substack{c=-W \\ m_c = J_{2g}+1}}^{W} \begin{bmatrix} S_0\left[|c|\right] & 0 \\ 0 & S_1\left[|c|\right] \end{bmatrix} \begin{bmatrix} D_t^{(0)}[m_c] \\ \left(D_t^{(1)}[m_c]\right)^* \end{bmatrix} \\ & \times P\left[\left\lfloor \frac{m_c}{2} \right\rfloor\right] \end{aligned} \tag{45}$$

where the index g is in the range $0 \leq g \leq N_j/2, m_u \triangleq (k+u)_N$ and $m_c \triangleq (k+c)_N$. In (45), the first and second summation parts are the pilot ICI noise from the subcarriers belong to the even and odd pilot index set, respectively.

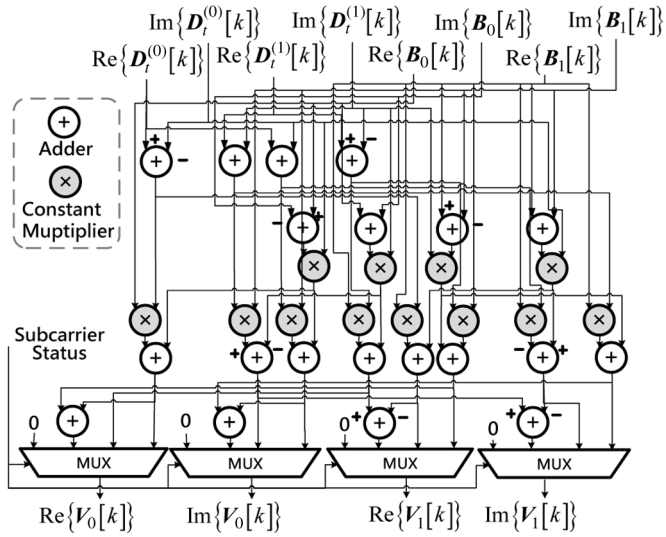

Fig. 9. STBC re-encoder circuit design.

B. STBC Re-Encoder

Complex multiplications are involved in (44) and (45). The implementation of a complex multiplier can be reduced from four multipliers and two adders to three multipliers and five adders. Since the data and pilot values have a constant value set, the complex multiplications in (44) and (45) can be implemented as constant multiplications. Hence, the STBC re-encoder contains 12 constant multipliers and 20 adders as shown in Fig. 9. Each constant multiplier can applythe canonic sign digit (CSD)expression and can be implemented by several adders. As shown in Fig. 9, the input $B_0[k]$ and $B_1[k]$ are the decision data or pilot symbols, and the outputs are selected according to the subcarrier status of the input signals.

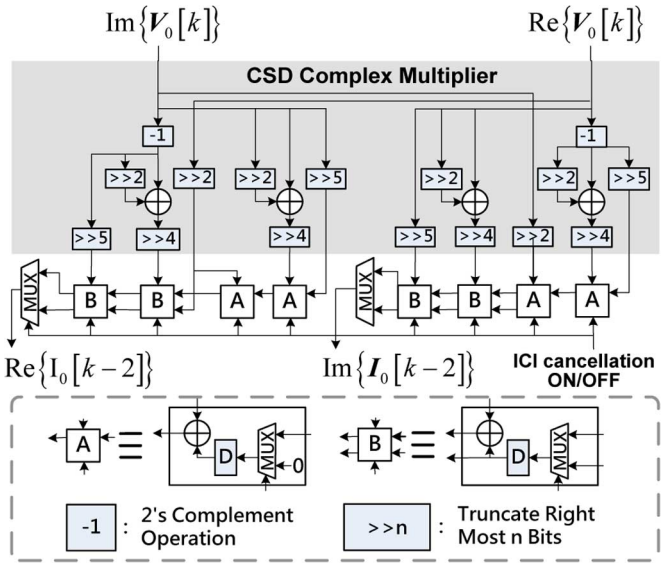

Fig. 10. Shaping filter circuit design for the first transmit antenna branch.

C. Interference Shaping Filter

We apply the CSD code on $\boldsymbol{S}_0$ and $\boldsymbol{S}_1$ to minimize the nonzero digits in the representation. The Doppler spread and the CCI noise can be approximated by multiplying the pre-computed weighting coefficients $\boldsymbol{S}_0$ and $\boldsymbol{S}_1$, as described in (41), (42), with the variation of noise-free received signal reconstructed by STBC re-encoder. Therefore, the complex multiplications in the interference shaping filter can be implemented as the constant CSD multiplications using only several adders. The shift registers are used to accumulate the ICI noises from the $2W$ neighboring subcarriers and the CCI noise from the same transmitted subcarrier. Fig. 10 illustrates the proposed circuit design.

D. Other STBC Signal Detection Methods

In this section, we briefly describe some other frequently referenced STBC signal detection methods including the ML method [3], the simplified maximum likelihood (SML) method [3], a LS method [4], a SIC method [4], and a diagonalized maximum likelihood decoder (DMLD) method [17].

1) ML Method and SML Method: From (14), the received signal can be expressed as

$$\boldsymbol{R}[k] = \widetilde{\mathbf{A}}[k]\boldsymbol{X}[k] + \boldsymbol{I}_{CCI}[k] + \boldsymbol{Z}'[k] \tag{46}$$

where $\boldsymbol{Z}'[\boldsymbol{k}]$ denotes the sum of $\boldsymbol{Z}[\boldsymbol{k}]$, $\boldsymbol{I}_{ICI}[k]$, and $\boldsymbol{I}_{ICI\Delta}[k]$. The ML method can be described as follows:

$$\widehat{\boldsymbol{X}}[k] = arg \min_{\hat{X}_F[k],\hat{X}_S[k]\in C_M} \left\| \boldsymbol{R}[k] - \mathbf{A}[k,k] \begin{bmatrix} \hat{X}_F[k] \\ \hat{X}_S[k] \end{bmatrix} \right\|^2 \tag{47}$$

where C_M denotes the constellation points. The ML method computes every possible combination of decision symbols and to select the most probable one.

The SML method stands for the signal detection method proposed by [3], and it does not estimate every combination of $\widehat{\boldsymbol{X}}[k]$ to solve (47) directly. Instead, it takes all constellation points as $\hat{X}_S[k]$ and subtract $\boldsymbol{I}_{CCI}[k]$ from $\boldsymbol{R}[k]$, and then it uses ML metrics as a criterion to decide $\hat{X}_F[k]$. Therefore, the SML method can reduce the computational complexity of the ML method from $|C_M|^2$ to $|C_M|$, where $|C_M|$ represents the number of constellation points.

2) LS Method and SIC Method: The LS method can be described as

$$\widetilde{\boldsymbol{X}}[k] = Dec\left\{\mathbf{A}^{-1}[k,k]\boldsymbol{R}[k]\right\}. \tag{48}$$

It takes the CFRs of two symbol intervals into account, so it has better performance than Alamouti's STBC method.

The SIC method introduces the ordered successive interference cancellation (OSIC) concept to improve the LS method. The complexity of the SIC is low, but it suffers error propagation if the first symbol decision is not correct.

3) DMLD Method: The DMLD method decouples two transmitted symbols by multiplying the received signal $\boldsymbol{R}[k]$ with a daigonalizing matrix as

$$\begin{bmatrix} \check{X}_F[k] \\ \check{X}_S[k] \end{bmatrix} = \begin{bmatrix} \left(H_1^{(0)}[k,k]\right)^* & H_0^{(1)}[k,k] \\ \left(H_1^{(1)}[k,k]\right)^* & -H_0^{(0)}[k,k] \end{bmatrix} \boldsymbol{R}[k]. \tag{49}$$

It detects symbols as

$$\widehat{X}_j[k] = arg \min_{\hat{X}_F[k],\hat{X}_S[k]\in C_M} \left\| \check{X}_j[k] - \chi[k]\hat{X}_j[k] \right\|^2 \tag{50}$$

where $\chi[k]$ denotes the negative determinant of the daigonalizing matrix.

The daigonalizing matrix reconstructs the orthogonality of the STBC code word, so the two symbols can be decoded separately. The DMLD method applies ML criterion to do the decoding. Therefore, it has good performance but high complexity.

V. Simulations and Design Results

The simulation results demonstrate the performance of the proposed STBC interference canceller based on the system described in Fig. 1. Since this paper is focused on the data detection as shown in Fig. 2, we assume that both timing and carrier frequency synchronization are perfect. The multipath channel adopts the International Telecommunication Union (ITU) Veh-A channel model with relative path power profiles of 0, -1, -9, -10, -15, and -20 (dB), and the path excess delays are uniformly distributed from 0 to 50 sampling periods which are smaller than the length of the CP. Jakes model is also used to generate Raleigh fading environment.

Several data detection schemes are defined in Table II. Both the software scheme (S2) and hardware scheme (H2)are based on the proposed CCI and ICI interference cancellation methods with different control parameters (C_T, C_C, C_I, C_D) as described in Fig. 2. The performance of the two-stage channel estimation (T0) is also provided for comparisons. Moreover, the performances of the perfect conditions P0, P1 and P2 are included for benchmarking. All schemes are simulated in floating point expect H2-fix. H2-fix is H2 scheme simulated in fixed point. Note that the output SNR at the STBC decoder defined in [8] is used as a gauge of the system performance to optimize the fixed-point word lengths in H2-fix. The word lengths of several

TABLE II
SIMULATED DECODING SCHEMES

Scheme Notation	Channel Estimation	CCI cancellation	ICI cancellation	Parameters (C_T, C_C, C_I, C_D)
P0	perfect	non	non	
T0 [8]	two-stage estimation			(4, 4, 4, 2)
P1	perfect	perfect	proposed 1st-order ICI modeling	
H2 (hardware scheme)	two-stage estimation	proposed CCI modeling		(3, 2, 3, 2)
S2 (software scheme)	two-stage estimation			(4, 2, 3, 2)
P2 (benchmark)	perfect	perfect	perfect	

TABLE III
WORD LENGTHS OF SEVERAL KEY SIGNALS IN THE PROPOSED STBC INTERFERENCE CANCELLER

Signal	Word Length
Stored previous CFR	8
CFR variation between two time slots	8
Decision symbol input of the STBC re-encoder	10
Output of the STBC re-encoder	10
Output of the interference shaping filter	11
Updated received signal	13

key signals in the proposed STBC interference canceller are summarized in Table III.

Fig. 11 shows the performance of 16 QAM modulation at the vehicle speed of 240 km/hr. The two-stage channel estimator provides very accurate CSI which performs almost equal to the perfect channel estimation, but the bounding floor at high SNR caused by interference noises is very obvious. With the aid of the proposed CCI and ICI interference cancellation methods in S2 and H2, the error floor phenomenon in T0 is significantly improved by about ten times. The performance of S2 shows that BER of 2×10^{-3} can be achieved in $\mathrm{E_b/N_0}$ of 30 dB. The H2 scheme has less data decision iterations than the S2 scheme. Although a high iteration operation in the proposed data decision scheme can have better performance, the timing requirement of a less iteration operation can be released to achieve low-cost design. The very small performance gap between H2 and S2 scheme indicates that the H2 scheme is an economic choice for hardware implementation. Moreover, the performance gap between H2 and H2-fix is less than 0.5 dB. We can conclude that the implementation method proposed in Section IV does not degrade the performance of the proposed algorithm. As compared with P1 and P2, S2 has only 0.4 dB and 3.5 dB performance gap in BER of 4×10^{-2}. Fig. 12 shows the performance of QPSK modulation at the vehicle speed of 240 km/hr. Our proposed S2 reduces the error floor of the two-stage channel estimator by about two times. BER of 3×10^{-4} can be achieved in $\mathrm{E_b/N_0}$ of 30 dB. Because QPSK modulation is very robust in noise interference, the differences among the performances of S2, H2, and H2_fix are very small. As compared with P1 and P2, S2 has only 2.0 dB and 2.8 dB performance gap in BER of 10^{-3}.

Several STBC data detection methods [3]–[6]have been briefly described in Section IV. Fig. 13 shows the BER performance of our proposed method and other methods at $\mathrm{E_b/N_0}$ of

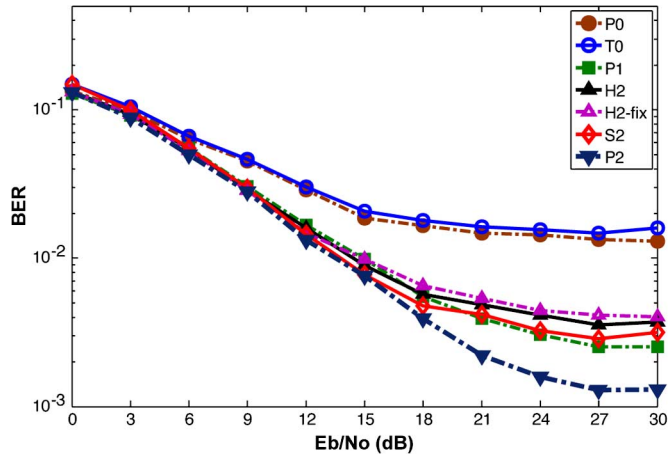

Fig. 11. BER performance for 16 QAM at the vehicle speed 240 km/hr.

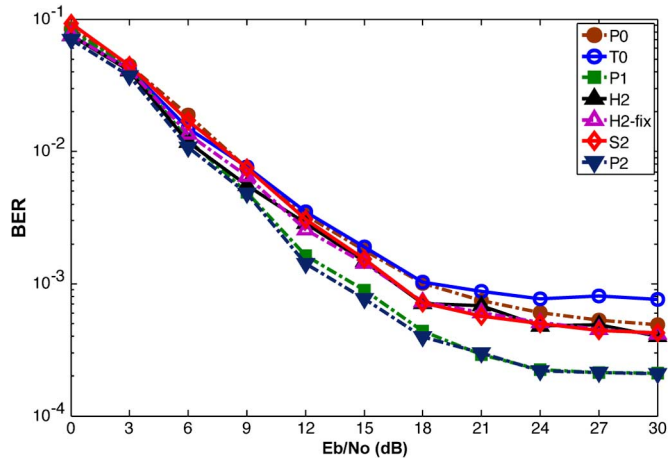

Fig. 12. BER performance for QPSK at the vehicle speed 240 km/hr.

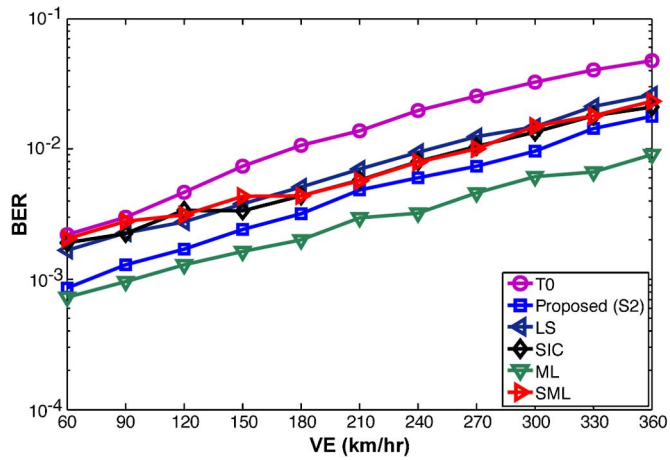

Fig. 13. BER performances versus the vehicle speed for 16 QAM.

16 dB. Note that the symbol-interval based CFRs is obtained by (24), (25) instead of the ideal channel estimation assumed in [3]. As shown in Fig. 13, our proposed scheme outperforms the other methods except the ML method at the vehicle speed of 240 km/hr and has similar performance at higher speed.

Table IV compares the computational complexities of one subcarrier data detection by using the proposed method and

TABLE IV
COMPUTATIONAL COMPLEXITIES OF OUR PROPOSED METHOD AND OTHER DATA DETECTION METHODS

Decoding Method	Variable Complex Multipliers	Constant Complex Multipliers	Complex Adders
Proposed	6	22	15
LS [4]	6	2	3
SIC [4]	12	3	4
ML [6]	$2(\lvert C_M\rvert)^2$	$4(\lvert C_M\rvert)^2$	$4(\lvert C_M\rvert)^2$
SML [3]	$2\lvert C_M\rvert$+6	$2\lvert C_M\rvert$	$2\lvert C_M\rvert$
DMLD [17]	$2\lvert C_M\rvert$+6	$2\lvert C_M\rvert$	$2\lvert C_M\rvert$+3

other methods [3]–[6], and [17]under our proposed system, where C_M denotes the number of constellation points. The complexity does not include that of the demapper and the channel estimation. A constant complex multiplier can be implemented as shift operations and additions, so it has considerably lower complexity than a variable complex multiplier. Although the ML data detection method has high performance, the complexity of the ML method is also significantly higher than other methods.

The detection methods [3]–[6], and [17]require the CFRs information of two symbol intervals of each time slot, e.g., $H_b^{(a)}[k,k]\ \forall a,b \in \{0,1\}$. In contrast, the proposed method requires only the average CFRs of each time slot. Hence, the channel estimator's computational complexity can be reduced by two times.

Moreover, other works are designed to reduce CCI, and they require extra decision feed-back technique, i.e., the sequential decision feedback sequence estimation (SDFSE) proposed in [6], to calculate ICI noise. However, our proposed method solves CCI and ICI problem jointly based on the same CFRs information. Therefore, our proposed method can has less computational complexity. As shown in Fig. 13 and Table IV, our proposed method requires low computation complexity and can provide high performance.

The CCI modeling in the proposed method is approximated from the averaged CFRs estimation in (24), (25). The extrapolation or interpolation results may be unreliable under fast fading channel since the temporal variation from symbol to symbol may be violent. Therefore, the performance of the CCI cancellation will be limited if the vehicle speed is very high.

The synthesis results are listed in Table V. The proposed STBC interference canceller is implemented in 90 nm 1P9MCMOS technology. The overall area of the proposed STBC interference canceller is 0.44 mm^2 and is equivalent to 109,299 gates. The proposed STBC-OFDM system samples the received signal at 11.2 MHz, and the STBC interference canceller operates at 83.3 MHz. The power is equivalent to 1.45 mW from 1 V supply voltage.

The ratio of combinational and non-combinational area is about 1:4; in other words, the usage of memory in this design occupies about 80% of the design. As shown in Fig. 8, the STBC decoder, the demapper, the received signal memories, and the memories storing the latest CFR estimations can be reused from the two-stage channel estimator. The overhead of our proposed interference canceller are the STBC re-encoder,

TABLE V
SYNTHESIS RESULTS OF THE PROPOSED STBC INTERFERENCE CANCELLER

Technology	CMOS 90nm	
Sampling Frequency	11.9 MHz	
Clock Frequency	83.3 MHz	
Two-stage Channel Estimator [8]		
SRAM Size (bits)	196.2K	
Total Area including SRAM (gates)	859,604 (3.43 mm^2)	
Power (mW)	43.71 @ 83.3 MHz	
Proposed STBC Interference Canceller		
	Overall	Overhead
SRAM Size (bits)	140.93K	22.14K
Total Area including SRAM (gates)	109,299 (0.44 mm^2)	42,277 (0.083 mm^2)
Power (mW)	1.45 @ 83.3 MHz	

the shaping filter, the dual-port memories for decision symbols, and the single-port memories used to store the CFR estimations of previous time slot. The STBC re-encoder and shaping filter take 11% of the STBC interference canceller. The overhead memories take 28% of the STBC interference canceller. Up to 61% of the hardware can be reused from the existed two-stage channel estimator design. After reusing with the two-stage channel estimator, the area requirement can be reduced to only 42,227 gates. As implemented in [8], the total gate count of the two-stage channel estimator is 859,604 gates. Our proposed STBC interference canceller takes only 4.9% overhead of the two-stage channel estimator, but the BER performance of this data detection scheme can behighly improved.

VI. CONCLUSION

In this paper, an STBC interference cancellation algorithm for ICI and CCI is proposed. We implement an efficient STBC interference canceller for an STBC-OFDM system in outdoor mobile channels. The proposed joint ICI and CCI canceller is successfully applied in an STBC-OFDM system with two transmit antennas and one receive antennas.

As compared with the performance of the two-stage channel estimator, the BER can be improved about 10 times by applying the proposed STBC interference cancellation for 16 QAM at the vehicle speed of 240 km/hr with $\mathrm{E_b/N_0}$ beyond 30 dB. The BER can achieve 2×10^{-3} without using channel coding.

The design of the proposed STBC interference canceller has an equivalent gate count of 109,299 gates, and 61% of which can be reused from the two-stage channel estimator. The design dissipates 1.45 mW at 83.3 MHz operating frequency using 90 nm CMOS technology with 1 V supply voltage. With verifications through design and simulation results, the proposed STBC interference canceller can provide a performance-improving solution for the STBC-OFDM systems in WMAN mobile wireless communication.

REFERENCES

[1] *Local and Metropolitan Area Networks Part 16: Air Interface for Fixed Broadband Wireless Access Systems*, IEEE Std 802.16-2004, Oct. 2004.

[2] *Local and Metropolitan Area Networks Part 16: Air Interface for Fixed and Mobile Broadband Wireless Access Systems*, IEEE Std 802.16e-2005, Feb. 2006.

[3] K. I. Lee, J. Kim, and Y. S. Cho, "Computationally efficient signal detection for STBC-OFDM systems in fast-fading channels," *IEICE Trans. Commun.*, vol. 90, no. 10, pp. 2964–2968, Oct. 2007.
[4] J. W. Wee, J. W. Seo, K. T. Lee, Y. S. Lee, and W. G. Jeon, "Successive interference cancellation for STBC-OFDM systems in a fast fading channel," in *Proc. IEEE Vehicular Technology Conf.*, Jun. 2005, vol. 2, pp. 841–844.
[5] J. Kim, B. Jang, R. W. Heath, Jr., and E. J. Powers, "A decision directed receiver for Alamouti coded OFDM systems," in *Proc. IEEE Vehicular Technology Conf.*, Oct. 2003, vol. 1, pp. 662–665.
[6] J. Kim, R. W. Heath, Jr., and E. J. Powers, "Receiver designs for Alamouti coded OFDM systems in fast fading channels," *IEEE Trans. Commun.*, vol. 4, no. 2, pp. 550–559, Mar. 2005.
[7] H. Hijazi and L. Ros, "Rayleigh time-varying channel complex gains estimation and ICI cancellation in OFDM systems," *Eur. Trans. Telecommun.*, vol. 20, pp. 782–796, 2009.
[8] H. Y. Chen, M. L. Ku, S. J. Jou, and C. C. Huang, "A robust channel estimator for high-mobility STBC-OFDM systems," *IEEE Trans. Circuits Syst. I*, vol. 57, no. 4, pp. 925–936, Apr. 2010.
[9] W. G. Jeon, K. H. Chang, and Y. S. Cho, "An equalization technique for orthogonal frequency-division multiplexing systems in time-variant multipath channels," *IEEE Trans. Commun.*, vol. 47, no. 1, pp. 27–32, Jan. 1999.
[10] L. Deneire, P. Vandenameele, P. van der Perre, B. Gyselinckx, and M. Engles, "A low-complexity ML channel estimator for OFDM," *IEEE Trans. Commun.*, vol. 51, no. 2, pp. 135–140, Feb. 2003.
[11] J. H. Park, M. K. Oh, and D. J. Park, "New channel estimation exploiting reliable decision-feedback symbols for OFDM systems," in *Proc. IEEE Int. Conf. Commun.*, Jun. 2006, vol. 7, pp. 3046–3051.
[12] M. L. Ku and C. C. Huang, "A refined channel estimation method for STBC/OFDM systems in high-mobility wireless channels," *IEEE Trans. Wireless Commun.*, vol. 7, no. 11, pp. 4312–4320, Nov. 2008.
[13] T. A. Lin and C. Y. Lee, "Predictive equalizer design for DVB-T system," in *Proc. IEEE Int. Symp. Circuits Syst.*, May 2005, vol. 2, pp. 940–943.
[14] H. Hijazi and L. Ros, "Polynomial estimation of time-varying multipath gains with ICI mitigation in OFDM systems," in *Proc. IEEE Int. Symp. Commun., Control and Signal Process.*, Mar. 2008, pp. 905–910.
[15] H. Hijazi and L. Ros, "Polynomial estimation of time-varying multipath gains with intercarrier interference mitigation in OFDM systems," *IEEE Trans. Vehicular Technol.*, vol. 58, no. 1, pp. 140–151, Jan. 2009.
[16] M. L. Ku, W. C. Chen, and C. C. Huang, "EM-based iterative receivers for OFDM and BICM/OFDM systems in doubly selective channels," *IEEE Trans. Wireless Commun.*, vol. 10, no. 5, pp. 1405–1415, May 2011.
[17] H. Kanemaru and T. Ohtsuki, "Interference cancellation with diagonalized maximum likelihood decoder for space-time/space-frequency block coded OFDM," in *Proc. IEEE Vehicular Technology Conf.*, May 2004, vol. 1, pp. 525–529.

Hsiao-Yun Chen received the B.S. degree in electronics engineering from Feng Chia University, Taichung, Taiwan, in 2002, the M.S. degree in electrical engineering from National Central University, Chung-Li, Taiwan, in 2004, and the Ph.D. degree in electronics engineering from National Chiao Tung University, Hsinchu, Taiwan, in 2009, respectively.

Her research interests include baseband signal processing, integrated circuit and system designs for wireless and mobile communications.

Wei-Kai Chang was born in Taipei, Taiwan, R.O.C. He received the B.S. and M.S. degrees in electronics engineering from National Chiao Tung University, Hsinchu, Taiwan, in 2008 and 2010, respectively.

His research interests include algorithm designs for wireless and mobile communications, integrated circuit design, and physical layer baseband signal processing.

Shyh-Jye Jou received the B. S. degree in electrical engineering from National Chen Kung University, Tainan, Taiwan, in 1982, and the M.S. and Ph.D. degrees in electronics from National Chiao Tung University, Hsinchu, Taiwan, in 1984 and 1988, respectively.

He joined Electrical Engineering Department of National Central University, Chung-Li, Taiwan, from 1990 to 2004 and became a Professor in 1997. Since 2004, he has been Professor of Electronics Engineering Department of National Chiao Tung University and became the Chairman from 2006 to 2009. Since August 2011 he has been the Vice President of Office of International Affairs, National Chiao Tung University. He was a visiting research Professor in the Coordinated Science Laboratory at University of Illinois, Urbana-Champaign during 1993–1994 and 2010 academic years. In the summer of 2001, he was a visiting research consultant in the Communication Circuits and Systems Research Laboratory of Agere Systems, USA. He has published more than 100 IEEE journal and conference papers. His research interests include design and analysis of high speed, low power mixed-signal integrated circuits, communication and bio-electronics integrated circuits and systems.

Prof. Jou was the Guest Editor of the IEEE JOURNAL OF SOLID-STATE CIRCUITS in November 2008. He received the Outstanding Engineering Professor Award from the Chinese Institute of Engineers in 2011. He served as the Conference Chair of IEEE International Symposium on VLSI Design, Automation and Test (VLSI-DAT) and International Workshop on Memory Technology, Design, and Testing. He also served as Technical Program Chair or Co-Chair in IEEE VLSI-DAT, International IEEE Asian Solid-State Circuit Conference, IEEE BIOMEDICAL CIRCUITS AND SYSTEMS, and other international conferences.